Journal of Statistical Physics, Vol. 98, Nos. 1/2, 2000

Multilayer Cooperative Sequential Adsorption

E. K. O. Hellén,[1] P. Szelestey,[2] and M. J. Alava[1, 3]

Received October 19, 1998; final September 14, 1999

Cooperative sequential adsorption is here extended to multilayer coverages. We discuss two different growth rules with cooperativity either restricted to only the first layer of coverage or applied in all layers. The unrestricted variant is considered in the case where lateral growth dominates over the nucleation of terraces. The limit of completely suppressed nucleation corresponds to a morphological transition to a flat interface from one governed by the Kardar–Parisi–Zhang equation. With the restricted growth rule we find interesting behavior resulting from a competition between lateral growth at the first layer and growth on the top of nucleated islands. There is an intermediate regime between random deposition at the submonolayer coverage and asymptotic random deposition behavior. In this regime the kinetic roughening can be studied by applying sequential adsorption rate equations for cluster lengths in the first layer, with an additional geometric argument.

KEY WORDS: Cooperative adsorption; kinetic roughening.

I. INTRODUCTION

Random sequential adsorption (RSA) and its close cousin cooperative sequential adsorption (CSA) have attracted some interest during the recent years as simple models of clustering.(1) One particular property of RSA and CSA models is that they can be formulated in terms of rate equations. These turn out to be exactly solvable in one spatial dimension due to the Markovian dynamics and the shielding property of empty sites.(2)

[1] Helsinki University of Technology, Laboratory of Physics, P.O. Box 1100, FIN-02015 HUT, Finland.
[2] Department of Theoretical Physics, Institute of Physics, Technical University of Budapest, H-1521 Budapest, Hungary.
[3] NORDITA, Blegdamsvej 17, DK-2100 Copenhagen, Denmark.

0022-4715/00/0100-0265$18.00/0

In the CSA model particles are deposited on a substrate so that the single-site coverage does not exceed unity. The fate of all particles depends on the neighborhood of the chosen destination. Both repulsive and attractive nearest-neighbor (NN) interactions can be considered. There is an apparent similarity—for the one-dimensional (1D) case—to polymer chain aggregation which was one of the early motives for the study of the CSA model.[3]

In this paper we discuss ways of extending the CSA model to multilayer growth (Multilayer CSA, MCSA). The motivation is based on noting the similarity between CSA-dynamics and the growth of surfaces by deposition.[4] MCSA might correspond to a solid interface that is formed by sticking of atoms from a gas phase; the sticking probability then depends among others on the local chemical environment of the adsorption site. The generalization of CSA to multilayer growth can naturally be done in several ways. We discuss two possible choices for the local growth rules corresponding to random deposition and the Kardar–Parisi–Zhang universality classes, respectively.

We introduce anisotropic and isotropic MCSA, which differ in whether the growth is cooperative only at the first layer of particles or, in general, at all times. There are variants of RSA—accelerated RSA—that have been developed to model chemisorption/physisorption phenomena, that are closely related to these ideas.[5]

The isotropic MCSA turns out to be similar to the polynuclear growth model[6] and to the square lattice variant of the Gates–Westcott model of polymer crystallization.[7, 8] In Section III, we discuss the therefore unsurprising fact that it belongs to the Kardar–Parisi–Zhang (KPZ) universality class.[9] There is a morphology/pinning transition that takes place when the attractive interaction between incoming particles and pre-existing steps wins completely over nucleation events at flat terraces. By studying the step densities in the steady state we are able to analyze the KPZ-nonlinearity near the transition.

The anisotropic case leads to a complicated version of random deposition-type growth with initial correlations, which we analyze by utilizing 1D rate equation theory. Using an extension thereof allows us to map the CSA timescale to that of kinetic growth, since in multilayer adsorption the concept of coverage differs from the original one. We combine geometric arguments with the rate equation solution for the cluster length distribution to study kinetic roughening in the regime where the coverage is small, but the height of a typical cluster is non-trivial (larger than unity). This phase shows interesting roughening properties that interpolate between the asymptotic, trivial random deposition limit and the likewise simple early stage, which is as well in the random deposition class of dynamics. Section V finishes the paper with conclusions.

II. MULTILAYER CSA—DEFINITIONS OF TWO MODELS

There are several ways of generalizing the CSA to multilayer growth. In MCSA the growth occurs by adding particles either on the substrate or on the top of previously deposited particles and the cooperativity of the local growth rules determines the universality class of the resulting interface. Here we consider the two natural choices for the rules leading to random deposition and KPZ type interfaces. The models are defined on a one-dimensional lattice of size L but the generalization to higher dimensions is straightforward.

In the isotropic MCSA the growth is cooperative at all layers and the dynamics equals to the growth rates

$$r = \begin{cases} q, & \text{no NNs in the lateral direction} \\ 1, & \text{otherwise} \end{cases} \tag{1}$$

With this choice of growth rules MCSA becomes a variable-rate deposition model with the local deposition rate being dependent on the local deposit structure. Figure 1a illustrates the isotropic growth rules.

The isotropic MCSA is identical to the discretized polynuclear growth model[6] and similar to the so-called Gates–Westcott model of polymer crystallization[7, 8] on a square lattice. It is also a simplification of the model studied earlier by Amar and Family,[10] without the restricted solid-on-solid (RSOS) condition which restricts the height difference between nearest neighbors to at most one. Their model was found to be of the Kardar–Parisi–Zhang universality class in $2+1$ dimensions.

In the random deposition multilayer cooperative sequential adsorption (RD-MCSA) the sticking of particles deposited on the substrate with no lateral nearest neighbors is inhibited in respect to particles landing elsewhere as illustrated in Fig. 1b. To be precise, the dynamics equates to the growth rates

$$r = \begin{cases} q, & \text{no NNs \& particle deposited on the substrate} \\ 1, & \text{otherwise, esp. for all particles in higher layers} \end{cases} \tag{2}$$

Physically, one could imagine this particular choice of rules to correspond to a deposit of material A being formed on a substrate of material B so that the sticking of A atoms on the substrate is inhibited with no neighbors of the same type. One could also use different rates r_i depending on the exact number of nearest neighbors. Our choice is a simplification. We also work within the range of $q \leqslant 1$, implying inhibition of cluster nucleation with respect to growth. Note in particular that one could also

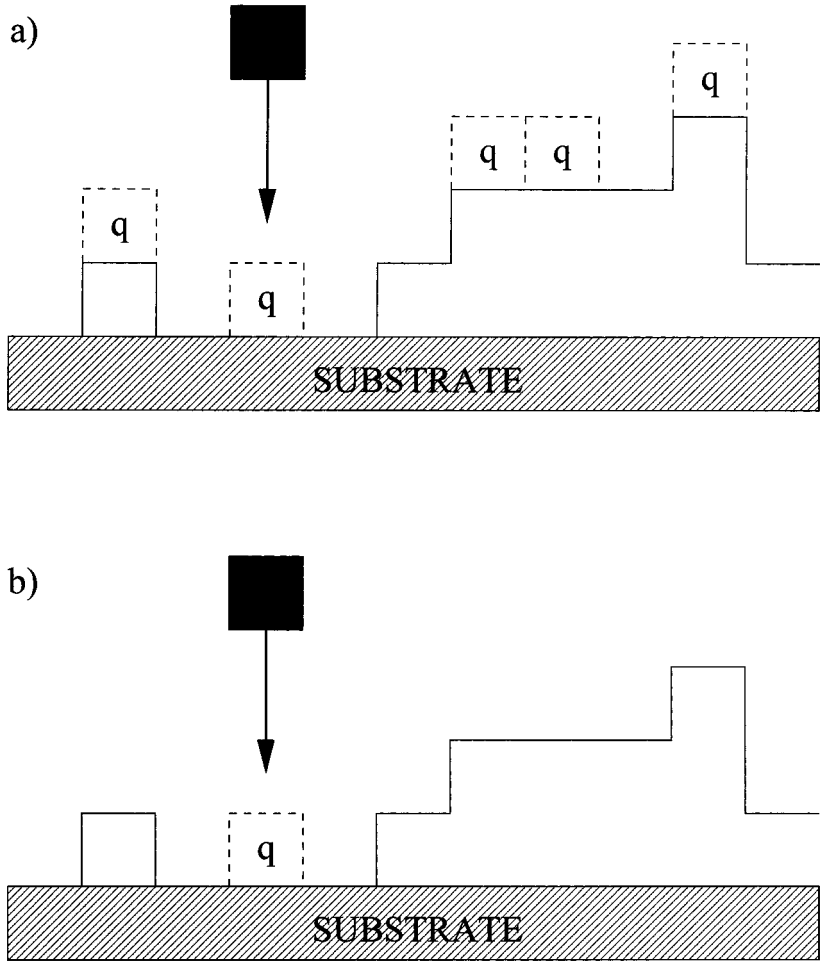

Fig. 1. (a) The isotropic and (b) the anisotropic growth rules for MCSA. The growth rate for unlabeled sites is unity and for labeled ones q.

consider other kinds of dynamics for particles *on the higher layers*. For example one could allow particles to diffuse on the top of islands that have already formed on the substrate.

In MCSA a particle or deposition event can be rejected and thus there are two natural timescales: that of coverage, measuring particles deposited per site, and that of deposition trials. These are not always directly related as is trivial to see. In studies of surface roughening time is usually measured using the coverage. For RD-MCSA, however, the interesting phenomena

happen at low coverages and the timescale of trials turns out to be more convenient for analytical purposes.

III. ISOTROPIC MCSA

The polynuclear growth model that is a close cousin of the isotropic MCSA belongs to the KPZ universality class.[11, 12] We checked the standard growth exponent β and the roughness exponent α for the isotropic MCSA by numerical simulations. The height–height difference correlation function in the saturated regime and the surface width yield $\beta = 0.32 \pm 0.02$, 0.32 ± 0.02, and 0.31 ± 0.02, and $\alpha = 0.50 \pm 0.02$, 0.49 ± 0.02 and 0.44 ± 0.02 for $q = 0.001$, 0.01, and 0.1, respectively. System size $L = 10^5$ and data are averaged over 50 samples. The values are consistent with the KPZ-exponents $\beta = 1/3$ and $\alpha = 1/2$.

The $q \to q_c = 0$ limit of the MCSA corresponds to a morphology/pinning transition: starting from an arbitrary configuration the surface equilibrates via domain wall/step annihilation till a steady state with $v = 0$ is reached. Here v is the average velocity of the interface defined as the number of particles in the system divided by the number of deposition attempts. Close but above the critical point we have that $v \sim (q - q_c)^\theta$, where θ defines the velocity exponent.[13] Similar considerations apply to growth processes in which adsorption competes with desorption.[14–16] It would be interesting to see how arbitrary initial configurations relax in the limit $q \to 0$.[12, 17, 18] We shall, however, discuss below the morphology transition near $q = 0$.

Simulations show that the step density saturates rapidly to a constant value. Thus the average terrace length $\bar{l}$ can be estimated in the steady state by considering a lattice gas model, in which steps nucleate in pairs in random positions and move apart with velocity V, which can be chosen to be one in our case. This approach is closely related to the analysis of the polynuclear growth model in one dimension.[6] Define $l(x)$ and $r(x)$ to be the densities of steps moving to the left and right, respectively, in the continuum limit where x denotes the spatial position. These densities satisfy the equations[6, 19, 20]

$$\frac{\partial l}{\partial t} = q + \frac{\partial l}{\partial x} - 2lr + \mu \tag{3}$$

$$\frac{\partial r}{\partial t} = q - \frac{\partial r}{\partial x} - 2lr + \mu \tag{4}$$

where μ is a noise term with $\langle \mu \rangle = 0$ and the product form of the annihilation terms reflects the fact that steps that annihilate each other are

uncorrelated. Let the total step density be $n = r + l$ and choose $l = r + m$ for a tilted surface with average tilt m which results in

$$\frac{\partial \langle n \rangle}{\partial t} = 2q - \langle n \rangle^2 + m^2 \tag{5}$$

Solving for $\bar{l} = \langle n \rangle^{-1}$ in the steady state gives

$$\bar{l}(q, m) = (2q + m^2)^{-1/2} \sim q^{-1/2} \tag{6}$$

Furthermore, the velocity is related to the average terrace length as $v = q + (1-q)\,\bar{l}^{-1} = q + (1-q)\sqrt{2q + m^2} \sim q^{1/2}$, which gives $\theta = 1/2$. This agrees with the solutions for the steady state of a corresponding spin chain-like model[8] and the Sine–Gordon chain.[12]

In the limit $q \to 1$ we expect the nonlinearity λ to vanish since at $q = 1$ the MCSA has a cross-over to the random deposition model. In the opposite limit $q \to 0$ the interface becomes pinned and analogously to the velocity λ diverges as $q^{-\phi}$.[21, 12, 17] The behavior can be analyzed in a standard fashion by using a screw boundary condition $h(L) = h(0) + Lm$ in the simulations.[4, 22] For small enough tilts the interface growth velocity depends quadratically on m. Thus expanding v around $m = 0$ and identifying the coefficient of the second order term with $\lambda/2$ leads to conclusion that $\lambda = (1-q)/\sqrt{2q} \sim q^{-1/2} \sim \bar{l}(q, 0)$ as $q \to 0$ and thus $\phi = 1/2$.

Figure 2 compares the predictions of the lattice gas theory with numerical simulations. It demonstrates that by using the scaling exponents derived, $\theta = \phi = 1/2$, we are able to collapse the numerical data into a single master curve. The inset includes both the theoretical prediction and simulation values for λ as a function of q. Apart from a constant offset the lattice gas result and the simulations for the growth velocity scale similarly with q ($\theta = 1/2$).

Note finally the differences between isotropic MCSA and earlier RSOS-growth models, for instance that by Amar and Family.[10] First, the isotropic MCSA can be analyzed in the small q limit using mean field arguments since there is no height difference restriction. Also, in our case λ should always be positive, since even an excess of left/right steps created by screw boundary conditions does not inhibit step nucleation.

IV. RANDOM DEPOSITION MCSA

A. Rate Equations for Cluster Lengths

In terms of standard growth models the anisotropic dynamics [Eq. (2)] translates into random deposition with correlations created by

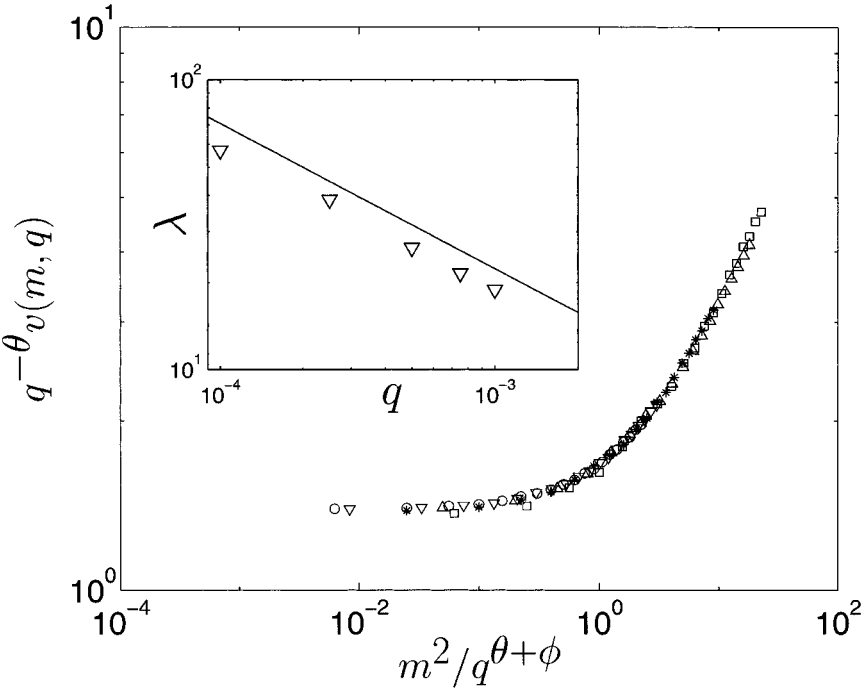

Fig. 2. A data collapse of the growth velocity data for various tilts m and for $q = 0.001$ (□), 0.00075 (∗), 0.0005 (○), 0.00025 (×), and 0.0001 (▽) using the theoretical values for the exponents $\theta = \phi = 1/2$. The inset shows the numerical values for λ and the theoretical curve $(1-q)/\sqrt{2q}$.

the first layer deposition dynamics that takes place on the substrate. Islands are free to grow in the transverse direction, but their coalescence takes place at a different rate compared to normal random deposition because of the difference in the growth rate for the first layer. This gives rise to a non-trivial cross-over phenomenon that persists as long as the substrate is not completely covered.

In the following we give a brief overview on the rate equation method which has turned out to be an efficient method for analyzing the CSA. The purpose is to show how the CSA rate equations can be used for analyzing the interface properties by relating the coverage to the deposition timescale and also present the appropriate approximations needed for the analysis in Section IV C. We concentrate on the early stages of cluster nucleation and growth of a partially filled first layer, in which case it is possible to study the kinetic roughening of the growing interface by combining the rate equation solution with geometric arguments for the shape of clusters.

Let n_s (n'_s) denote the probability of finding a cluster of filled (empty) sites of length s per lattice site. The number of particles per lattice site that one *tries* to deposit in the system is τ. This parameterization of time by deposition trials is a key point in the calculations, which enables one to solve the rate equations. On the other hand, in the studies of interface roughening time is measured using the coverage, which can be solved once the number of rejected particles as a function of τ is known. Although τ is simply proportional to real time, we prefer to use the symbol t for coverage as usually done in interface studies. Below, we derive a relation between the two timescales. This is because we are interested in the growth properties (e.g., the growth exponent β) as a function of the coverage, not as a function of τ. Note that the analysis differs from standard treatments of CSA since the single site coverage is allowed to exceed unity and the growth takes place in $1+1$D. Thus a cluster of length s in general consists of more particles than just s.

In the thermodynamic limit the rate equations read[23]

$$\frac{\partial n_1}{\partial \tau} = q \sum_{s=1}^{\infty} s n'_{s+2} - 2n_1 \tag{7}$$

$$\frac{\partial n_k}{\partial \tau} = 2n_{k-1}\left(1 - \frac{n'_1}{\delta}\right) + n'_1 \sum_{s=1}^{k-2} \frac{n_s n_{k-s-1}}{\delta^2} - 2n_k \tag{8}$$

$$\frac{\partial n'_1}{\partial \tau} = 2n'_2 + 2q \sum_{s=3}^{\infty} n'_s - n'_1 \tag{9}$$

$$\frac{\partial n'_k}{\partial \tau} = 2n'_{k+1} + 2q \sum_{s=k+2}^{\infty} n'_s - 2n'_k - (k-2)\, q n'_k \tag{10}$$

where $k > 2$, $\delta = \sum_s n'_s = \sum_s n_s$, and n_s and n'_s fulfill the relations

$$\sum_{s=1}^{\infty} s n_s = p \tag{11}$$

$$\sum_{s=1}^{\infty} s n_s + \sum_{s=1}^{\infty} s n'_s = 1 \tag{12}$$

where p is the fraction of filled sites in the first layer. The number of rejected particles $R(\tau)$ can be obtained with $R(0) = 0$ from

$$\frac{\partial R}{\partial \tau} = (1-q) \sum_{s=1}^{\infty} s n'_{s+2} \tag{13}$$

The length distribution of empty clusters needed in equation (13) can be solved exactly[24]

$$n_1'(\tau) = 2(1-p_0)\, e^{-\tau} \int_0^\tau e^x (1-e^{-qx})(e^{qx}-1+q)\, \zeta(x)\, \mathrm{d}x \tag{14}$$

$$n_k'(\tau) = (1-p_0)\, e^{(3-k)\,q\tau} (1-e^{-q\tau})^2\, \zeta(\tau) \tag{15}$$

where p_0 is the fraction of occupied sites in the beginning and $\zeta(x) = \exp\{2(1-1/q)(e^{-qx}+qx-1)-3qx\}$. Inserting the solutions (14) and (15) to equation (13) gives

$$R(\tau) = (1-p_0)(1-q) \int_0^\tau \zeta(x)\, \mathrm{d}x \tag{16}$$

resulting in an exact relation between the time τ and the coverage $t(\tau) = \tau - R(\tau)$. By writing and solving the rate equations as a function of τ and regarding it only as a parameter simplifying the calculations, and using equation (16) it is possible to get the cluster length distribution as a function of coverage, too.

A formal solution of the length distribution of filled clusters is also possible but the expressions become very complicated even for small values of k[23, 1] thus prohibiting even numerical evaluation. To study the interface roughening in the non-trivial small coverage limit we have to approximate n_k. When both q and p are small the coalescence of clusters is negligible and we make a rough approximation that clusters do not coalesce at all, i.e., $n_1'(\tau) = 0$, $\tau \geqslant 0$. This allows us to write equations (7) and (8) in matrix form as

$$\frac{\partial \mathbf{n}(\tau)}{\partial \tau} = Q\mathbf{n}(\tau) + \mathbf{q}(\tau) \tag{17}$$

where $\mathbf{n}(\tau) = [\, n_1(\tau)\, n_2(\tau)\, n_3(\tau) \cdots \,]^T$, $Q_{ij} = 2(\delta_{i+1,\,j} - \delta_{i,\,i})$, $\mathbf{q}(\tau) = [\, q\zeta(\tau)\, 0\, 0 \cdots \,]^T$, and $\delta_{i,\,j}$ is the Kronecker delta. The solution of equation (17) is

$$\mathbf{n}(\tau) = e^{\tau Q} \left[\int_0^\tau e^{-xQ} \mathbf{q}(x)\, \mathrm{d}x + \mathbf{n}(0) \right] \tag{18}$$

which can be written out as

$$n_k(\tau) = e^{-2\tau} \sum_{i=1}^{k} \frac{(2\tau)^{k-i}}{(k-i)!} \left[n_i(0) + \frac{(-2)^{i-1}}{(i-1)!}\, q \int_0^\tau x^{i-1} e^{2x} \zeta(x)\, \mathrm{d}x \right] \tag{19}$$

We would like to know $p(\tau)$, $\langle n(\tau)\rangle$ and $\langle n(p)\rangle$, where $\langle n\rangle$ stands for the average cluster length. The first one can be obtained with the help of equations (11), (12) and (15) exactly as

$$p(\tau) = 1 - n_1'(\tau) - (1-p_0)(2e^{q\tau} - 1)\,\zeta(\tau) \tag{20}$$

where $n_1'(\tau)$ is given by equation (14). In order to calculate $\langle n(\tau)\rangle$ we use

$$p(\tau) = \sum_{s=1}^{\infty} n_s(\tau)\langle n\rangle \equiv (n_0 + N_a - N_c)\langle n\rangle \tag{21}$$

which gives

$$\langle n(\tau)\rangle = \frac{1 - n_1'(\tau) - (1-p_0)(2e^{q\tau} - 1)\,\zeta(\tau)}{n_0 + N_a(\tau) - N_c(\tau)} \tag{22}$$

where $n_0 = \sum_{s=1}^{\infty} n_s(0)$ and N_a (N_c) is the average number of new (coalesced) clusters. For $N_a(\tau)$ we get almost the same differential equation as for $R(\tau)$ and $N_a(\tau) = qR(\tau)/(1-q)$.

The simplest way to calculate the number of coalesced clusters N_c is to modify the equations (9) and (10) so that clusters can not coalesce. In this case we get for isolated empty clusters by omitting the term n_1' from Eq. (9)

$$\tilde{n}_1'(\tau) = 2(1-p_0)\int_0^{\tau} (1 - e^{-qx})(e^{qx} - 1 + q)\,\zeta(x)\,\mathrm{d}x \tag{23}$$

and the number of coalesced clusters can be calculated as $N_c(\tau) = \tilde{n}_1'(\tau) - n_1'(\tau)$, which completes the solution (22). We were not able to invert equation (20) for $\tau(p)$ and thus calculate $\langle n(p)\rangle$ analytically, but equations (20) and (22) implicitly give the solution just using τ as a parameter.

B. Behavior of Cluster Growth

Figure 3 shows the number of rejected particles per lattice site as a function of the actual coverage $t = \tau - R(\tau)$. Simulations confirm the theoretical result [Eq. (16)] and in particular show that there is a crossover coverage above which the growth velocity becomes constant. This coverage decreases with q. Figure 4 and its inset discuss the average length of a cluster $\langle n(t)\rangle$. It is interesting to note that the average mass per

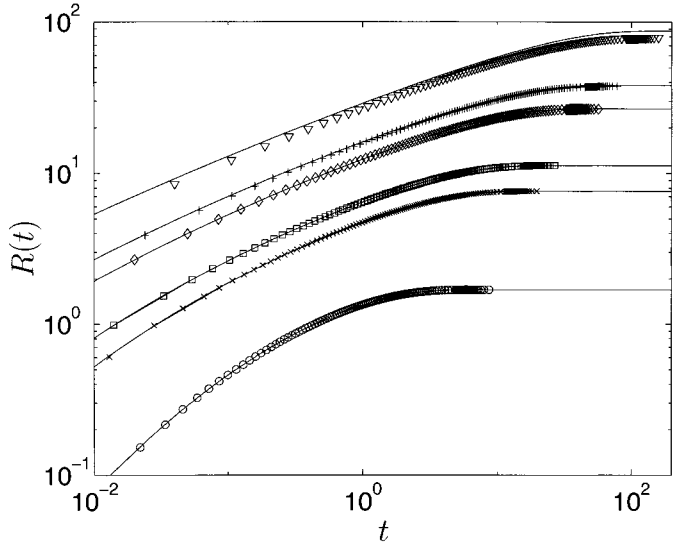

Fig. 3. The number of rejected particles per site (R) as a function of coverage for $q = 0.1$ ($\bigcirc$), 0.01 ($\times$), 0.005 ($\square$), 0.001 ($\diamond$), 0.0005 ($+$), and 0.0001 ($\triangledown$) from simulations. The lines are analytical results from Eq. (16).

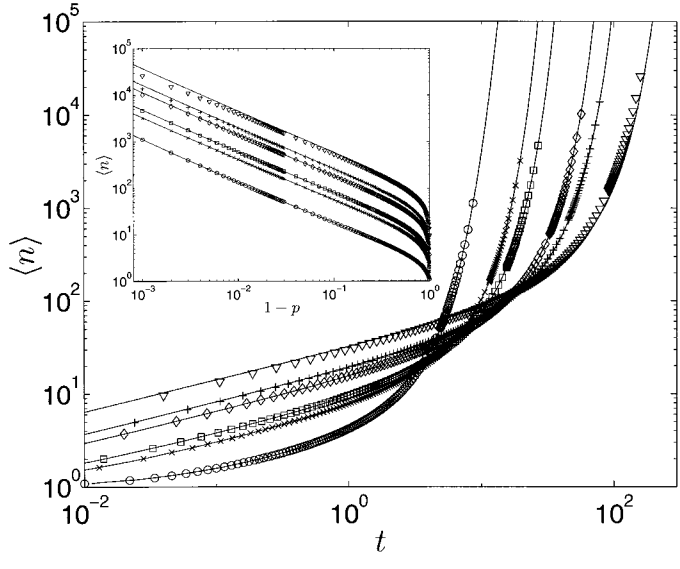

Fig. 4. The average cluster length $\langle n \rangle$ vs. the coverage t for the same q-values as in Fig. 3. The inset shows the average cluster length vs. the fraction of the substrate still unoccupied by deposited particles $(1-p)$. In both figures the solid lines are theoretical values from equations (20) and (22).

cluster is for small coverages largest for small q whereas the opposite becomes the case once the cluster length diverges. The inset shows in addition that the cluster length scales with the fraction of the substrate covered with the deposit, p, (in the sense of percolation theory) as expected close to the critical point of 1D site percolation: $\langle n \rangle \sim (1-p)^{-1}$.[25]

C. Surface Roughness in RD-MCSA

The expected scaling of the interface roughness in RD-MCSA is a combination of early time effects when the anisotropic growth rules still play a role and late time random deposition behavior. Figure 5 shows two

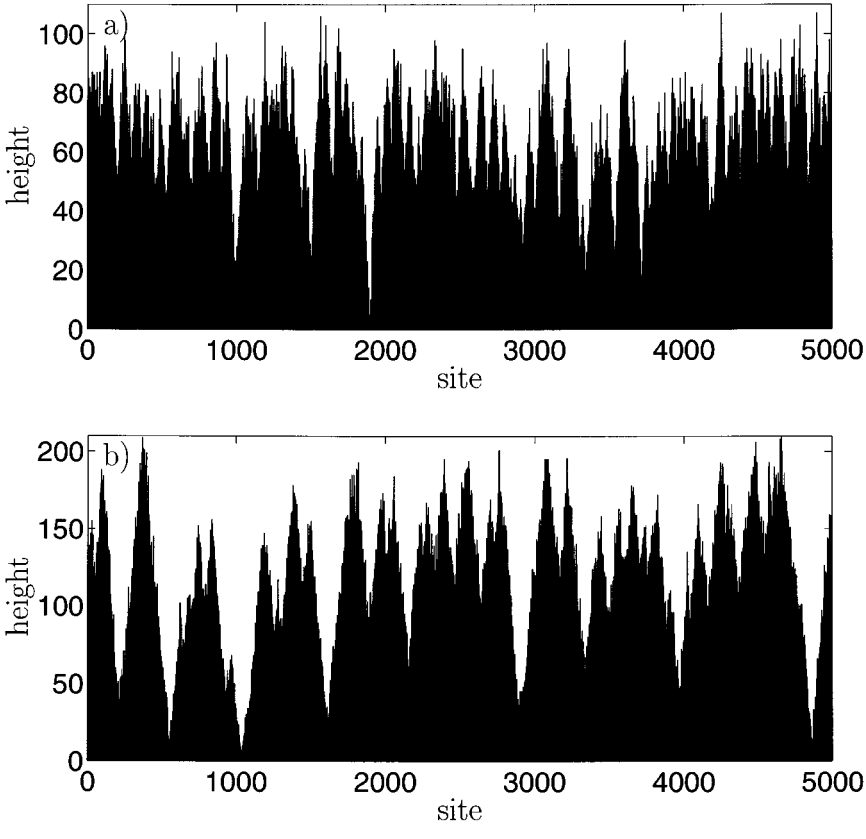

Fig. 5. Two different surface configurations for RD-MCSA at the time when the substrate is just fully covered: (a) $q = 0.001$, $t \approx 57$ and (b) $q = 0.0001$, $t \approx 109$. System size $L = 5000$.

examples of how the surface morphology looks like at late times, in the random deposition regime but with correlations from the initial phase. As $t \to \infty$ these effects vanish.

For small enough t such "hat-like" morphologies are however important with respect to the surface roughening. It is easy to see that the RD-MCSA growth rules amount to that a single cluster grows in a statistically homogeneous way so that the lateral and transverse growth velocities are the same. The complications arise from cluster coalescence (see Fig. 5b).

We now utilize the fact that for small q and p a single cluster has a generic shape of a triangle, whose height on the average is half of its width. Using this we can relate the density of heights to cluster lengths as

$$h_k(\tau) = \tfrac{1}{2} n_{2k-2}(\tau) + n_{2k-1}(\tau) + \tfrac{3}{2} n_{2k}(\tau) + 2 \sum_{s=2k+1}^{\infty} n_s(\tau) \tag{24}$$

and calculate the first and second moments numerically from Eq. (24) as a function of τ using Eq. (19). Thus we obtain the surface width $w(t(\tau)) = \sqrt{\langle h(t)^2 \rangle - \langle h(t) \rangle^2}$ using τ again as an implicit parameter. The simulations show that the growth exponent β characterizing the surface width in the early time regime ($w \sim t^{\beta}$) is not a constant. It has an approximate value that grows from 0.5 to approximately 0.6 during the formation of the first few layers. This can be compared with the value that would result from the single-cluster dynamics ($\bar{\beta} = 1$). The difference between $\bar{\beta}$ and the real β is, similarly to the change in the exponent, due to the competition between the random deposition like nucleation events and the cooperative growth of the previously nucleated islands. Note that the $\langle h \rangle \ll 1$ behavior is just typical of standard random deposition: there are no complications as all the clusters have $h_j = 0$, $j > 1$. The solution of the surface width from Eq. (24) reproduces the numerical work (Fig. 6).

V. CONCLUSIONS

The aim of this paper has been to discuss the extensions of monolayer cooperative sequential adsorption to multilayer growth. We have studied two different cases, corresponding to analogues of the Kardar–Parisi–Zhang and random deposition universality classes, respectively. In general both of these growth models imply that the local growth rate depends on the neighborhood of the site considered.

In the isotropic MCSA formulation the growth rules are of the KPZ universality class. Nevertheless, there are interesting details in the strongly inhibitory regime, close to $q = 0$. By studying the growth dynamics in a

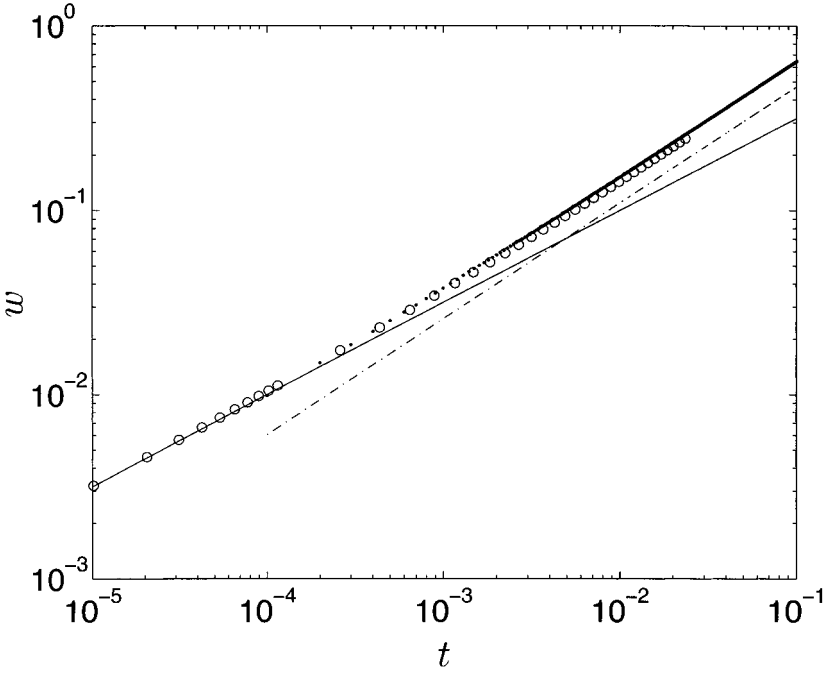

Fig. 6. Early-time surface roughening in the RD-MCSA. Numerical data (•) and analytical result (○) for the surface width for $q = 0.001$. The solid and dash-dotted lines have slopes 1/2 and 0.63, respectively, and are guides for the eye.

lattice gas formulation for steps, one can derive the KPZ-nonlinearity λ as a function of q, the growth parameter. This allows to find the "depinning"-type morphology transition exponent in the neighborhood of $q = 0$ for λ, which, as well as the velocity exponent θ, attains the value of 1/2. The result is related to polynuclear growth, the dynamics of driven Sine–Gordon chains,[12] and traffic models. Indeed, the isotropic MCSA maps to a traffic model/driven diffusive system with three kinds of particles (holes, "positive" and "negative" charges).

More interestingly, the RD-MCSA has a cross-over phase to the standard random deposition problem. This is entirely governed by the early stage CSA dynamics. We have used standard CSA theory to account for the formation statistics of clusters in the $1 + 1$D case, which can be treated analytically. Relating the timescale of the trials in the CSA formulation to the usual coverage based timescale in the surface roughening allows a discussion of the early-time roughening before the random deposition-kind behavior sets in. To our knowledge, this is the only model which shows re-entrant behavior with three phases: early random deposition-like

roughening, a cross-over phase with non-trivial properties, and final random deposition-class characteristics. An interesting extension would be to consider other choices for the dynamics in the higher layers. This would change the average morphology of individual clusters—for the RD-MCSA the mean shape is that of a triangle—but might keep the problem still analytically tractable.

It would be interesting to study the MCSA in the same limits in the $2+1$ dimensional case. In the anisotropic formulation it is easy to see that at low q the model would give rise to a "fattening" percolation cluster: for initial stages of growth the deposit has the 2D projection of a CSA percolation cluster,[26, 27] the voids inside which would be filled slowly compared to transverse growth. The actual growth dynamics are however related to the poorly-understood question of shielding configurations in normal multidimensional CSA and thus analytic progress would seem prohibitive. In the limit in which a small fraction of the substrate has been covered it might be possible to utilize polynuclear growth-type continuum limit ideas.[28] In $2+1$D it is also possible that using different growth rates for sites with different coordination numbers might give rise to interesting phenomena, as one can tune this to e.g., change the surface tension of the droplets on the surface.

For isotropic MCSA the $2+1$D-limit has already been explored by Amar and coworkers in the RSOS-type case. Nevertheless, the pinning transition close to $q=0$ exists in arbitrary dimensions as well as the cross-over effects close to $q=1$. As the morphology of islands in greater dimensions than $1+1$ becomes much more complicated it would seem less likely that one could hope to find the scaling exponents by similar simple arguments as in $1+1$D. Indeed, the existence of stationary states of growth is as such a very complicated question, as shown recently by Gates and Westcott for the $2+1$D case.[29]

ACKNOWLEDGMENT

We thank J. Kertész for comments about the manuscript.

REFERENCES

1. J. W. Evans, *Rev. Mod. Phys.* **65**:1281 (1993).
2. J. W. Evans, D. K. Hoffmann, and D. R. Burgess, *J. Chem. Phys.* **80**:936 (1984).
3. J. B. Keller, *J. Chem. Phys.* **37**:2584 (1962); J. B. Keller, *J. Chem. Phys.* **38**:325 (1963); T. Alfrey, Jr. and W. G. Lloyd, *J. Chem. Phys.* **38**:318 (1963); C. B. Arends, *J. Chem. Phys.* **38**:322 (1963).
4. A.-L. Barabási and H. E. Stanley, *Fractal Concepts in Surface Growth* (Cambridge University Press, 1995).

5. G. J. Rodgers and J. A. N. Filipe, *J. Phys. A*: *Math. Gen.* **30**:3449 (1997).
6. W. van Saarloos and G. Gilmer, *Phys. Rev. B* **33**:4927 (1986).
7. D. J. Gates and M. Westcott, *Proc. R. Soc. Lond. A* **416**:443 (1988).
8. D. J. Gates and M. Westcott, *Proc. R. Soc. Lond. A* **416**:463 (1988).
9. M. Kardar, G. Parisi, and Y.-C. Zhang, *Phys. Rev. Lett.* **56**:889 (1986).
10. J. G. Amar and F. Family, *Phys. Rev. Lett.* **64**:543 (1990).
11. J. Krug, P. Meakin, and T. Halpin-Healy, *Phys. Rev. A* **45**:638 (1992).
12. J. Krug and H. Spohn, *Europhys. Lett.* **8**:219 (1989).
13. L.-H. Tang and H. Leschhorn, *Phys. Rev. A* **45**:R8309 (1992); S. V. Buldyrev, A.-L. Barabási, F. Caserta, S. Havlin, H. E. Stanley, and T. Vicsek, *Phys. Rev. A* **45**:R8313 (1992).
14. J. Kertész and D. Wolf, *Phys. Rev. Lett.* **62**:2571 (1989).
15. U. Alon, M. Evans, H. Hinrichsen, and D. Mukamel, *Phys. Rev. Lett.* **76**:2710 (1996).
16. H. Hinrichsen, R. Livi, D. Mukamel, and A. Politi, *Phys. Rev. Lett.* **79**:2710 (1997).
17. J. Krug and H. Spohn, *Phys. Rev. A* **38**:4271 (1988).
18. P. L. Krapivsky and E. Ben-Naim, *Phys. Rev. E* **56**:3788 (1997).
19. F. C. Frank, *J. Cryst. Growth* **22**:233 (1974).
20. N. Goldenfeld, *J. Phys. A: Math. Gen.* **17**:2807 (1984).
21. L. A. N. Amaral, A.-L. Barabási, and H. E. Stanley, *Phys. Rev. Lett.* **73**:62 (1994).
22. J. Krug and H. Spohn, in *Solids Far from Equilibrium*, C. Godrèche, ed. (Cambridge University Press, 1991).
23. J. J. González and K. W. Kehr, *Macromolecules* **11**:996 (1978).
24. J. J. González, P. C. Hemmer, and J. S. Høye, *Chem. Phys.* **3**:228 (1974).
25. J. W. Evans, J. A. Bartz, and D. E. Sanders, *Phys. Rev. A* **34**:1434 (1986).
26. S. R. Anderson and F. Family, *Phys. Rev. A* **38**:4198 (1988).
27. D. E. Sanders and J. W. Evans, *Phys. Rev. A* **38**:4186, (1988).
28. E. Ben-Naim and P. L. Krapivsky, *Phys. Rev. E* **56**:6680 (1997).
29. D. J. Gates and M. Westcott, *J. Stat. Phys.* **81**:681 (1995).